Science of the Total Environment 807 (2022) 150817

Contents lists available at ScienceDirect

Science of the Total Environment

journal homepage: www.elsevier.com/locate/scitotenv

Microglial phagocytosis of polystyrene microplastics results in immune alteration and apoptosis *in vitro* and *in vivo*

Wookbong Kwon [a,b,1], Daehwan Kim [a,b,1], Hee-Yeon Kim [b,c], Sang Won Jeong [a], Se-Guen Lee [a], Hyun-Chul Kim [a], Young-Jae Lee [a], Mi Kyung Kwon [a], Jun-Seong Hwang [a], Jee Eun Han [c], Jin-Kyu Park [c], Sung-Jun Lee [a,*], Seong-Kyoon Choi [a,b,**]

[a] Division of Biotechnology, DGIST, Daegu, Republic of Korea
[b] Core Protein Resources Center, DGIST, Daegu, Republic of Korea
[c] College of Veterinary Medicine, Kyungpook National University, Daegu 41566, Republic of Korea

HIGHLIGHTS

- PS-MP oral treatment was sufficient for brain deposition *via* microglial phagocytosis.
- PS-MP induces microglial morphological change, immunes responses, and apoptosis.
- PS-MPs altered immune response, immunoglobulins, and microRNAs clusters expression.
- PS-MPs changes microglial differentiation and apoptotic markers and NF-κB activation.

GRAPHICAL ABSTRACT

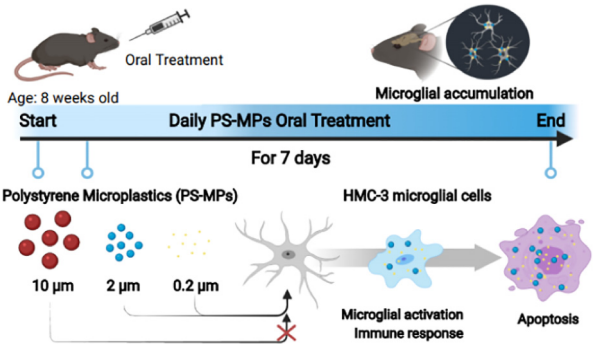

ARTICLE INFO

Article history:
Received 21 June 2021
Received in revised form 18 September 2021
Accepted 1 October 2021
Available online 7 October 2021

Editor: Kevin V. Thomas

Keywords:
Polystyrene microplastics
Mouse
Brain
Microglia
Immune response
Apoptosis

ABSTRACT

The remarkable increase in plastic usage and widespread microplastic (MP) pollution has emerged as a substantial concern today. Many recent studies have revealed MPs as potentially hazardous substances in mammals. Despite several reports on the impact of small MPs in the brain and behaviors in aquatic animals, it is still unclear how small MPs affect the brain and its underlying cellular physiology in terrestrial animals. In this study, we investigated the accumulation of polystyrene MPs (PS-MPs) in mouse brain after oral treatment using three types of fluorescent PS-MPs of different sizes (0.2,2 and 10 μm). We found that PS-MPs were deposited in microglial cells of the brain. Following differential treatment of PS-MPs in human microglial HMC-3 cells, we identified changes in cellular morphology, immune responses, and microglial apoptosis induced by phagocytosis of 0.2 and 2 μm PS-MPs. By analyzing the PS-MP-treated HMC-3 cell transcriptome, we showed that PS-MPs treatment altered the expression of clusters of immune response genes, immunoglobulins, and several related microRNAs. In addition, we confirmed alterations in microglial differentiation marker expression with the activation of NF-κB, pro-inflammatory cytokines and apoptotic markers in PS-MP-treated human microglial cells and in mouse brain. Our findings suggest a potential risk of small PS-MPs in microglial immune activation, which leads to microglial apoptosis in murine and human brains.

* Correspondence to: S.-J. Lee, Division of Biotechnology, DGIST, Daegu 42988, Republic of Korea.
** Correspondence to: S.-K. Choi, Core Protein Resources Center (CPRC), Division of Biotechnology, DGIST, Daegu 42988, Republic of Korea.
E-mail addresses: schrisj@dgist.ac.kr (S.-J. Lee), cskbest@dgist.ac.kr (S.-K. Choi).
[1] These authors contributed equally to this work.

https://doi.org/10.1016/j.scitotenv.2021.150817
0048-9697/

1. Introduction

Over the decades, the earth has been contaminated with numerous different types of plastics following the remarkable increase in plastic production, utilization, and indiscriminate dumping (Rochman and Hoellein, 2020). Among the various problems caused by discarded plastics, microplastics (MPs), plastic-derived particle sizes <5 mm are becoming a major issue in marine, soil, and atmospheric environments (Barnes et al., 2009; Lee and Hur, 2020). They can float in air, be inhaled through the respiratory system, and contained in water, which is easily absorbed by many aquatic animals that we eat (Akanyange et al., 2021; Rivoira et al., 2020; Sussarellu et al., 2016; Ward et al., 2019). Positioning as a top consumer of the aquatic food chain, MPs can be ingested through fresh water and MP-containing seafood (Mercogliano et al., 2020). Therefore, there is growing concern regarding the risk of MPs being absorbed by humans.

A number of studies have shown that MP accumulation in various tissues of aquatic animals, including intestinal organs, liver, gonads, and brain, affects inflammatory and reproductive activity and induces abnormal behaviors (Lu et al., 2016; McCormick et al., 2020; Qiang and Cheng, 2021; Suman et al., 2020; Sussarellu et al., 2016; Umamaheswari et al., 2020; Wang et al., 2020; Yang et al., 2020). In studies of polystyrene MPs (PS-MPs), which account for the largest proportion of aquatic and soil MP pollution, treatment of land animals such as mice revealed PS-MP deposition in the gut, liver, and gonads, leading to inflammation, colitis, and reproductive toxicity (Hou et al., 2021; Li et al., 2020; Lu et al., 2018; Xie et al., 2020). Moreover, there have been a number of reports concerning the accumulation of MPs in mouse brain and MP treatment experiments in human neuronal cells (Deng et al., 2018; Estrela et al., 2021; Prüst et al., 2020). However, neurotoxic studies regarding the effects of MPs in the human brain are, however, mostly limited to *in vitro* studies that do not show the intake process and physiological responses of our brain to MP exposure.

To better understand the physiological mechanisms and outcomes involved in MP intake in the brain, we designed and performed 1-day and 1-week oral treatments of PS-MPs in mice (Fig.1A). We found that PS-MPs were deposited not only in the kidney and gut, but also in the brain, and co-localized with microglial markers. After PS-MP treatment of human microglial HMC-3 cells, we identified phagocytosis and morphological changes in microglia in response to treatment with PS-MPs < 2 μm in size. In addition, we evaluated transcriptional alterations to clusters of immune response genes, immunoglobulins, and several microRNAs resulting from PS-MP exposure of microglial HMC-3 cells. Finally, comparing brain samples after 1-day and 1-week of exposure, we found microglial activation against early PS-MPs exposure, which eventually led to apoptosis subsequent to chronic PS-MPs exposure. Our findings suggest a novel potential process involving PS-MPs deposition in the brain conducted by microglial phagocytosis, and present new insights into the health risks posed by PS-MPs in the brain.

2. Material and methods

2.1. PS-MPs

Three types of round-shape fluorescently-labelled PS-MPs (1.0% *w*/*v*) with a particle size of 0.2 μm (yellow, FP-0252-2), 2 μm (nile blue, FP-2065-2), or 10 μm (nile red, FP-10056-2) were purchased from Spherotech, Inc. (Lake Forest, IL, USA). The detailed information of PS-MPs used in the experiments can be found in the manufacturer's instruction. PS-MP solutions were prepared with phosphate buffered saline (PBS) or relevant culture media, stored in the dark, and administrated after vortexing.

2.2. Animals

Eight-week-old C57BL/6 mice ($n = 6$ per group; Orient Bio, Seongnam, Korea) were orally administered 200 μL of PS-MPs (0, 2.5, and 10 μg/mL) by oral administration. The concentration of PS-MPs treatment was determined following several previous *in vivo* studies (Stock et al., 2019; Yang et al., 2019). Half of the mice were sacrificed 24 h after the first administration, while the remainder were sacrificed after 7 further consecutive oral administrations of PS-MPs. The brain, kidney, and gut were dissected and prepared for the experiments described in Fig. 1A. All animal experiments were performed following the guidelines and permission from the Daegu Gyeongbuk Institute of Science and Technology Laboratory Animal Resource Center (DGIST LARC).

2.3. Cell culture

Human microglial HMC-3 cells, purchased from the ATCC, were maintained in minimum essential medium (MEM) (Gibco, Waltham, MA, USA) supplemented with 10% fetal bovine serum (FBS) (Hyclone, Marlborough, MA, USA) and 1% penicillin/streptomycin (Gibco). All cells were incubated at 37 °C under a 5% CO_2 atmosphere.

2.4. Cell viability assay

Cell Counting Kit-8 (CCK-8) (Dojindo, Rockville, MD, USA) was used to determine cytotoxicity. HMC-3 cells were seeded in 96-well plates at a density of 3×10^3 cells/well and treated with 0.2, 2, or 10 μm-sized PS-MPs at concentrations of 1, 5, or 10 μg/mL. After 24 and 48 h, CCK-8 solution was added to each well and incubated for 60 min. Optical density was measured at 450 nm using a SpectraMax iD3 microplate reader (Molecular Devices, San Jose, CA, USA). The relative optical density of each treatment group was compared with that of the untreated control group.

2.5. Cell cycle analysis

Cell cycle analysis was performed using propidium iodide (PI) staining (Invitrogen, Carlsbad, CA, USA). HMC-3 cells treated with PBS or 10 μg/mL of mixed PS-MPs were incubated for 24 h at 37 °C under a 5% CO_2 atmosphere. After the detachment of whole cells using trypsin-ethylenediaminetetraacetic acid (EDTA) (Gibco), followed by two washes with PBS and 100% ethanol fixation for 1 h, cells were washed twice with PBS and incubated with 500 μL PI solution (1 mg/mL PI and 10 mg/mL RNase A (ThermoFisher Scientific, Waltham, MA, USA) (Devriese et al., 2015; Sharifinia et al., 2020)), and 0.5% Triton X-100 (Generay Biotech, Shanghai, China) in a darkened incubator for 15 min at 37 °C. Cells were then analyzed using a BD Accuri C6 flow cytometer (BD Biosciences, San Jose, CA, USA). At least 20,000 events were recorded for each sample.

2.6. Apoptosis assays

HMC-3 cells were treated with PBS or 10 μg/mL of mixed PS-MPs for 24 h at 37 °C under a 5% CO_2 atmosphere. Cells were then harvested and stained with the Dead Cell Apoptosis Kit with Annexin V Alexa Fluor™ 488 and PI (Invitrogen). Cells were analyzed using a BD Accuri C6 flow cytometer (BD Biosciences), and at least 10,000 events were acquired per sample.

For fluorescent apoptotic cell imaging, HMC-3 cells treated with PBC or 10 μg/mL of o.2 or 2 μm PS-MPs for 8 or 24 h were stained using apoptosis assay kit (ab176749, Abcam) following manufacturer's instruction.

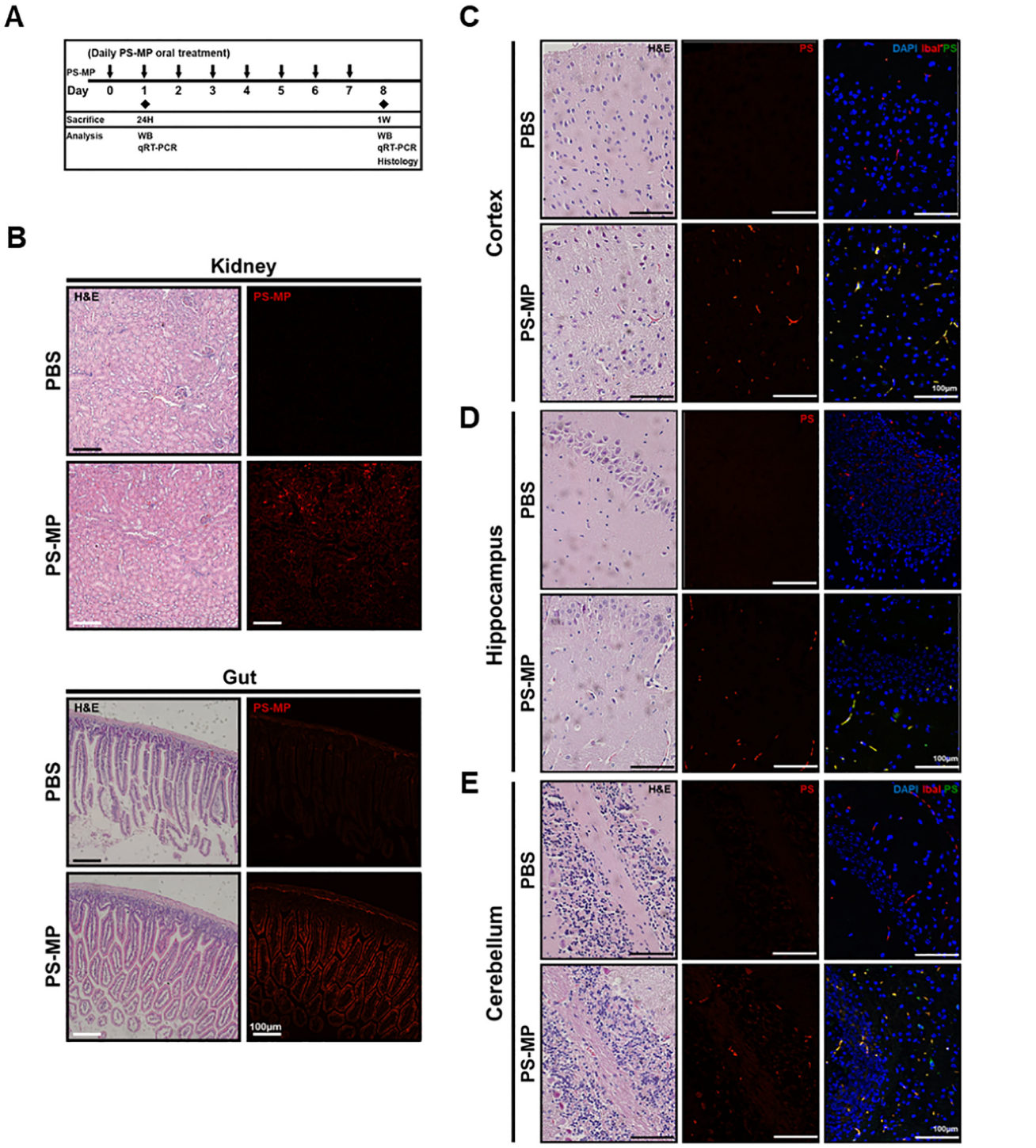

Fig. 1. PS-MPs accumulation in kidney, gut, and cortical, hippocampal, and cerebellar regions of the brain after PS-MPs oral administration in mice. (a) Schematic diagram illustrating the experimental schedule for PS-MPs oral treatment in mice. (b) Representative H&*E*-stained or fluorescent images of kidney and gut from mice orally treated with PS-MPs for 7 consecutive days. Scale bar = 100 μm. (c–e) Representative images of H&E-stained (left panel), PS-MPs, or PS-MPs with Iba1 (right panel) staining from cortex (c), hippocampus (d), and cerebellum (e) of mice orally treated with PS-MPs for 7 consecutive days. Scale bar = 100 μm.

2.7. Confocal imaging

HMC-3 cells were plated on confocal microscopy dishes at a density of 3×10^4 cells/plate and individually treated with 0.2, 2, or 10 μm PS-MPs at a concentration of 10 μg/mL. 24 h after individual PS-MP treatments, cells were washed with PBS, fixed with 4% paraformaldehyde (PFA), and incubated with 1% bovine serum albumin (BSA) in PBS-T containing 0.2% Triton X-100 for blocking non-specific binding. Cells were then stained with a primary antibody against IbaI (#019–19; FUJIFILM Wako, Neuss, Germany) overnight at 4 °C. After washing three times with PBS-T for 10 min each, cells were incubated with Alexa488 (A11001; ThermoFisher Scientific) or Alexa594 (A11037; ThermoFisher Scientific) secondary antibodies for 3 h in a darkened chamber followed by mounting with DAPI-containing Vectashield (Vector Laboratories, Burlingame, CA, USA). Images were acquired and analyzed using a FV1200 confocal microscope (Olympus, Tokyo, Japan).

2.8. Live cell imaging

3×10^4 HMC-3 cells were seeded into a confocal microscopy dish and treated with 10 μg/mL of mixed PS-MPs. For 24 h, images of the live cells were taken every hour using an FV1200 confocal live cell microscope (Olympus) at 37 °C 5% CO_2.

2.9. Western blot analysis

Protein lysates of PS-MP-treated HMC-3 cells or dissected brain samples from PS-MP-treated mice were prepared using Proprep lysis buffer (Intron Biotechnology, Seongnam, Korea). Protein concentrations were determined using the Bradford protein assay (Bio-Rad, Hercules, CA, USA). Protein lysates were separated by gel electrophoresis using 4%–15% Mini-PROTEAN® TGX™ Precast Protein Gels (Bio-Rad) and transferred to nitrocellulose membranes (Bio-Rad). After blocking with 5% BSA in TBS-T containing 0.2% Tween 20 (Biorad), primary antibodies against IbaI (#019–19; FUJIFILM Wako), CD68 (ab201340; Abcam, Cambridge, UK), CD16 (SC-58962; Santa Cruz Biotechnology, Dallas, Texas, USA), CD206 (PA5–101657; Invitrogen), STAT3 (#12540; Cell Signaling Technology), phospho-STAT3 (#9145; Cell Signaling Technology), NF-κB (#8242; Cell Signaling Technology), phospho-NF-κB (#3039; Cell Signaling Technology), Survivin (#5023; Cell Signaling Technology), Bax (#5023; Cell Signaling Technology), PARP (#9532; Cell Signaling Technology), cleaved-PARP (#5625; Cell Signaling Technology), Caspase8, cleaved-Caspase8, Caspase3 (#9662; Cell Signaling Technology), cleaved-Caspase3 (#9664; Cell Signaling Technology), and β-actin (sc-47,778; Santa Cruz Biotechnology) were incubated overnight at 37 °C. After three washes with TBS-T, secondary anti-rabbit (#7074 s; Cell Signaling Technology) or anti-mouse IgG (sc-5,161,002; Santa Cruz Biotechnology) antibodies labelled with horseradish peroxidase were incubated for 2 h at room temperature. Using the Clarity Western ECL substrate (#1705061; Bio-Rad) signals were developed, and protein expression was visualized using the ImageQuant LAS500 system (GE Healthcare, Uppsala, Sweden).

2.10. Real-time quantitative polymerase chain reaction (qPCR)

cDNA samples of the PS-MP-treated brain tissue or HMC-3 cells were synthesized from extracted RNA using the MiniBEST Universal RNA extraction kit (#9767; Takara, Shiga, Japan), according to the manufacturer's instructions. With TB Green Premix EX Taq (Takara), RT-qPCR was performed using the StepOnePlus RT-qPCR system (ThermoFisher Scientific). Relative mRNA expression was measured using the $2^{-\Delta\Delta Ct}$ method (Livak and Schmittgen, 2001). The following primers were used in RT-qPCR analysis: *iNOS* (forward, 5′-TTC AGT ATC ACA ACC TCA GCA AG-3′; reverse, 5′-TGG ACC TGC AAG TTA AAA TCC C-3′), *IL-1β* (forward, 5′-AGC TAC GAA TCT CCG ACC AC-3′; reverse, 5′-CGT TAT CCC ATG TGT CGA AGA A-3′), *TNF-α* (forward, 5′-CCT CTC TCT AAT CAG CCC TCT G-3′; reverse, 5′-GAG GAC CTG GGA GTA GAT GAG-3′), *CCL2* (forward, 5′-CAG CCA GAT GCA ATC AAT GCC-3′; reverse, 5′-TGG AAT CCT GAA CCC ACT TCT-3′), *IL-6* (forward, 5′-ACT CAC CTC TTC AGA ACG AAT TG-3′; reverse, 5′-CCA TCT TTG GAA GGT TCA GGT TG-3′), *TGF-β* (forward, 5′-CAG CAA CAA TTC CTG GCG ATA-3′; reverse, 5′-AAG GCG AAA GCC CTC AAT TT-3′), and *GAPDH* (forward, 5′- CAG CCT CAA GAT CAT CAG CA-3; reverse, 5′-TGT GGT CAT GAG TCC TTC CA-3′).

2.11. Microarrays

GeneChip analysis was conducted with HMC-3 cells treated with PBS, 2.5 or 10 μg/mL of mixed PS-MPs. Expression data were analyzed using ExDEGA (EBIOGEN Inc., Seoul, Korea).

2.12. Statistical analysis

All experimental data are presented as means ± SD of triplicate samples from at least three independent experiments. Mean differences were analyzed using Student's *t*-test, and *p*-values <0.05, were considered statistically significant.

3. Results

3.1. Bioaccumulation of PS-MPs in mouse kidney, gut, and cortical, hippocampal, and cerebellar brain regions after orally-administered PS-MPs

As a number of previous studies have shown that short-term MP exposure can lead to MP deposition in several organs (Stock et al., 2019; Yang et al., 2019), we designed a 7-day oral PS-MP treatment experiment and checked the accumulation of PS-MPs in the kidney and gut by histological analysis (Fig.1A, B). The concentration of the To further evaluate particle accumulation in the brain, we histologically analyzed the brain after 7 days of treatment and confirmed PS-MP bioaccumulation in the cortex, hippocampus, and cerebellum of the mouse brain (Fig.1C-E). Interestingly, we found that the brain-deposited PS-MPs were co-localized with Iba1, a marker of microglia, in all three regions of the brain (Fig. 1C-E, right panel).

3.2. PS-MP deposition and its effects in HMC-3 cells differ with PS-MP exposure time

Since we checked the bioaccumulation of PS-MPs in several brain regions using microglial markers, we next investigated whether the PS-MPs were actually deposited inside the microglial cells. To that end, we first treated human microglial HMC-3 cells with three types of PS-MPs of different sizes (0.2, 2, and 10 μm). We found that 0.2- and 2-, but not 10-μm sized PS-MPs, were deposited inside the HMC-3 cells after 24 h of treatment (Fig. 2A). Microglial PS-MPs were deposited in the cytosol of HMC-3 cells. In cell viability assays performed using CCK-8 assays, three types of PS-MPs were used at different concentrations (1, 5, and 10 μg/mL) for 24, 48, or 72 h. Interestingly, we found that the optical density of HMC-3 cells treated with 0.2 and 2 μm PS-MPs for 24 h was significantly increased in a concentration-dependent manner; however, there were no specific changes in the optical density of 10 μm-treated HMC-3 cells at 24 h treatment time point (Fig. 2B). In contrast to the 24 h treated group, the relative O·D value of cells after treatment with PS-MPs for 48 h or 72 h were substantially declined regardless of PS-MPs size differences (Fig. 2C). To further investigate whether the increased HMC-3 cell proliferation after 24 h PS-MPs treatment was related to alterations in cell cycle distribution, we conducted flow cytometric analysis after PI staining (Fig. 2D). As a result, we observed that the G0/G1 phase of PS-MP-treated cells was slightly decreased ($p = 0.077$), while the M phase ratio was slightly increased in PS-MP-treated HMC-3 cells ($p = 0.070$) (Fig. 2E). These results suggested that microglial ingestion of PS-MPs < 2 μm in size initially affected cell proliferation but eventually diminished proper HMC-3 cell proliferation.

3.3. Phagocytosis and subsequent apoptosis of HMC-3 cells after PS-MPs treatment

To better understand the accumulation of PS-MPs and their underlying processes and responses in microglial cells, we next evaluated morphological changes to HMC-3 cells after PS-MP treatment by conducting live cell imaging. Throughout the 24 h live cell imaging, we observed microglial phagocytosis of the PS-MPs (indicated with blue arrows), morphological changes in microglia cells after PS-MP ingestion (indicated by green arrows), and early apoptotic morphology of HMC-3 cells (indicated with red arrows) (Fig. 3A). These morphological changes were also observed in HMC-3 cells treated with 0.2 or 2 μm

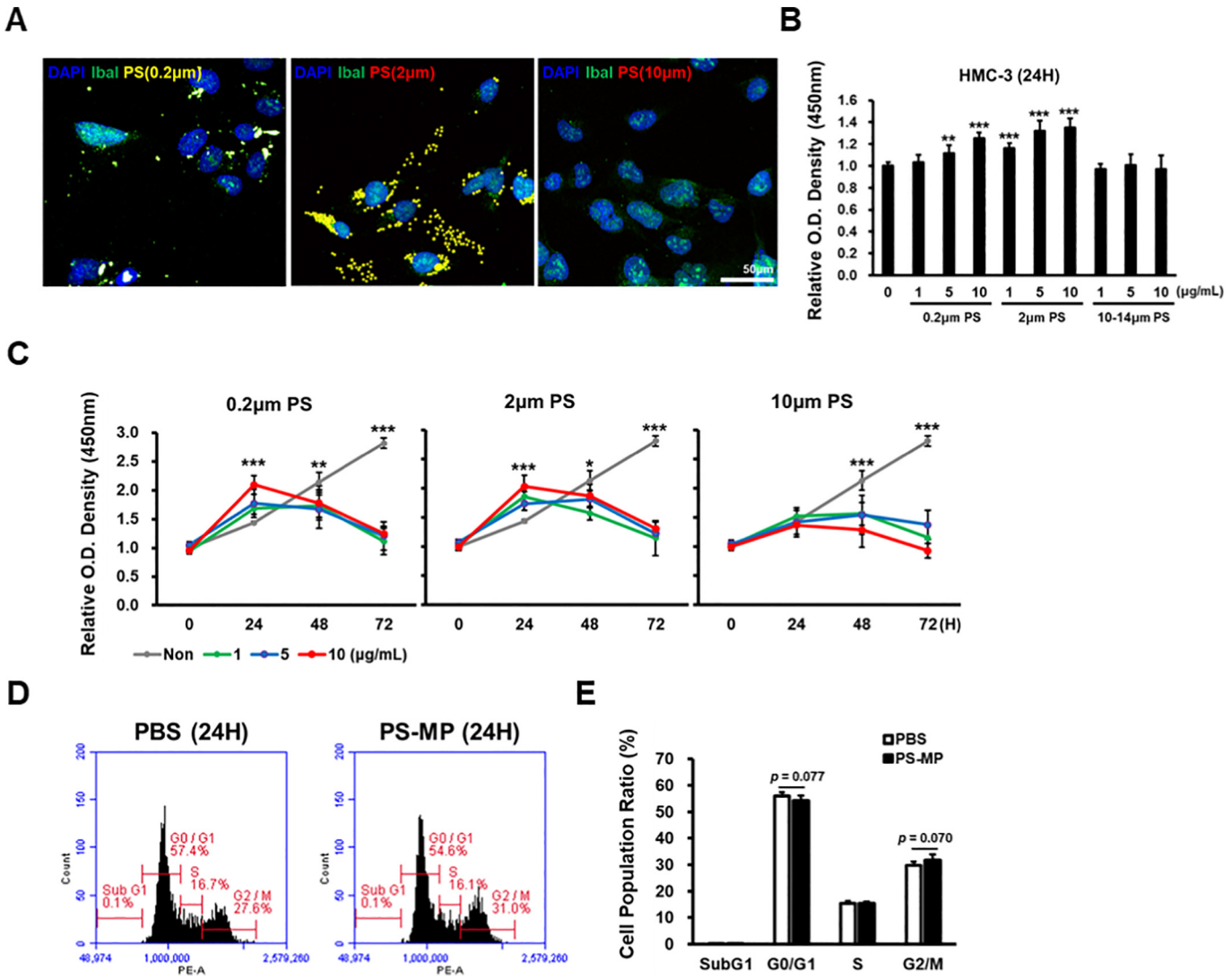

Fig. 2. Accumulation of PS-MPs in HMC-3 cells after treatment with three different sized PS-MPs. (a) Representative images of Iba1 immunostained HMC-3 cells treated with 0.2, 2, or 10 μm PS-MPs. Scale bar = 50 μm. (b-c) Cell viability as assessed by CCK-8 assays in HMC-3 cells treated with PBS, 0.2, 2, or 10 μm PS-MPs at concentrations of 1, 5, or 10 μg/mL. Relative optical density at 450 nm was measured 24 h (b) or 24, 48, and 72 (c) after PS-MPs treatment. (d) Representative images of cell cycle analysis from HMC-3 cells treated with 10 μg/mL of mixed PS-MPs for 24 h examined by BD Accuri C6 flow cytometry. (e) Cell population ratio of each group of cells analyzed from cell cycle analysis. $^{**}p < 0.01$, $^{***}p < 0.001$ compared to the control group.

PS-MPs for 24 h; we observed swollen amoeboid-shaped microglial cells (green arrows) as well as cells in the process of apoptosis (red arrows) (Fig. 3B). To confirm the apoptotic morphology of microglial HMC-3 cells after PS-MPs treatment, we measured apoptotic cell rates by flow cytometry using Annexin V and PI staining (Fig. 3C). We found that the number of late apoptotic cells, not early apoptotic cells, was significantly increased after exposure to PS-MPs for 24 h, implying that 24 h was sufficient time for HMC-3 cells to engulf PS-MPs and proceed to further cellular processes (Fig. 3D). Through western blotting analysis of several apoptotic marker proteins, we verified the induction of microglial apoptosis after 24 h of PS-MPs treatment, and observed a marked decrease in levels of the anti-apoptotic marker survivin, with remarkable elevation of pro-apoptotic marker proteins including Bax, cleaved-PARP, cleaved-Caspase 8, and cleaved-Caspase 3 (Fig. 3E). To clearly confirm the apoptotic change by PS-MPs treatment in HMC-3 cells, we checked the live/apoptotic fluorescence of cells and evaluated increased apoptosis with morphological changes in HMC-3 cells against 0.2 or 2 μm PS-MPs treatment (Fig. 3F). Through these data, we identified microglial phagocytosis of PS-MPs < 2 μm in size and subsequent apoptotic progress after 24 h of exposure.

3.4. Microglial activation and immune responses after PS-MPs treatment in HMC-3 cells

Despite the concentration-dependent increase in viability of HMC-3 cells after 24 h of PS-MPs treatment (Fig. 2), the cells also exhibited a substantial increase in apoptosis (Fig. 3). Microglial cells are known to change their cellular phenotypes at various stages in response to stimuli such as central nervous system injuries, cellular debris, external factors, and so on; they can be polarized into M1 or M2 phenotypes (Hu et al., 2015; Lan et al., 2017). To further define this change in microglial phenotype upon PS-MP exposure, we next examined the microglial cell type markers CD68, CD16, and CD206, by performing western blotting. After 24 h of treatment with 0.2 or 2 μm PS-MPs, HMC-3 cells displayed increased Iba1 expression, as expected (Fig. 4A). Moreover, the protein expression level of the microglial activation marker CD68 was markedly elevated by PS-MPs treatment of HMC-3 cells. This increasing tendency remained for the M1-type marker CD16 and the M2-type marker CD206 (Fig. 4A). We next examined the activation of two major microglial immune response signals and identified that phosphorylation of STAT3 and NF-κB proteins was clearly increased by PS-MPs treatment

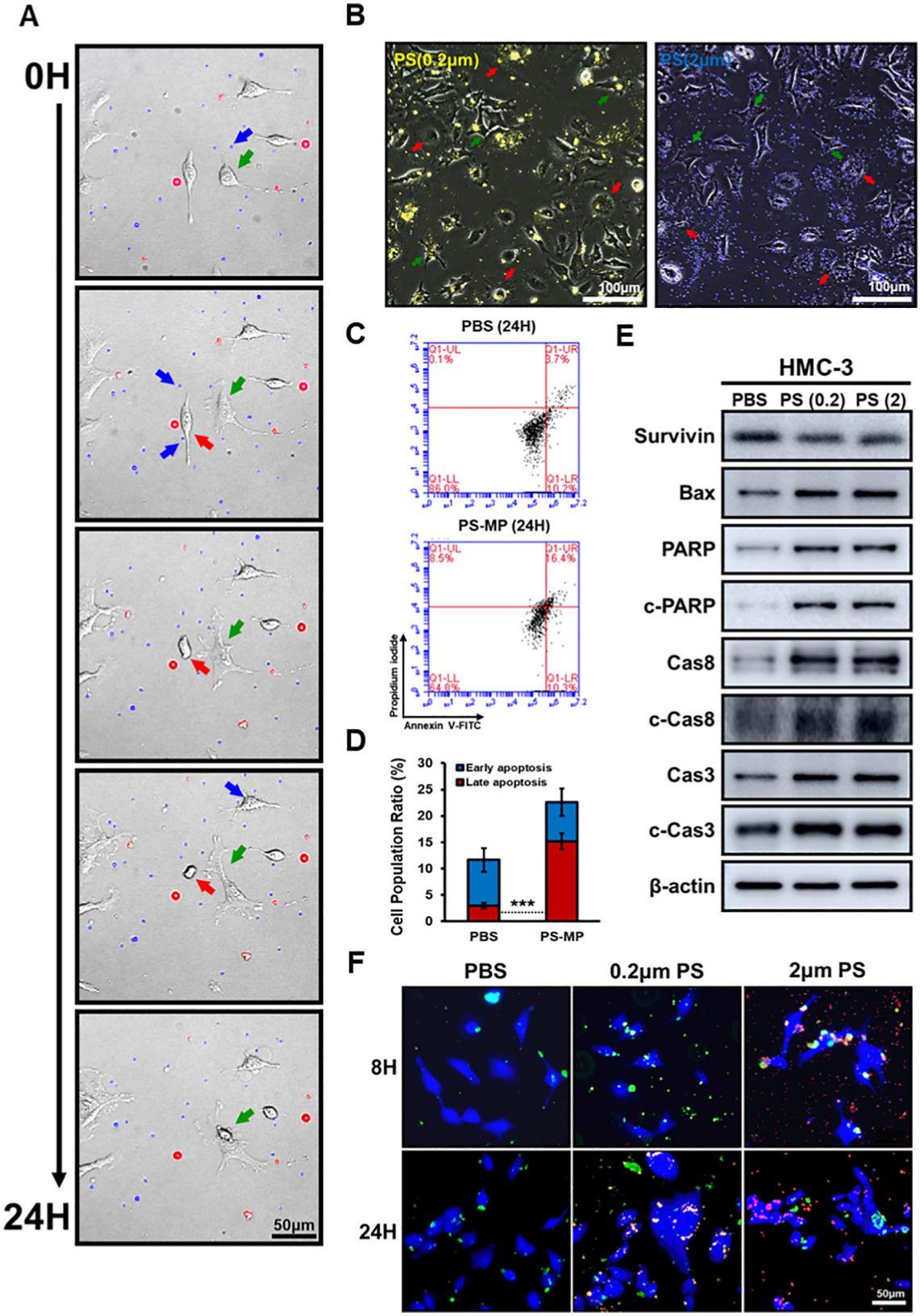

Fig. 3. Microglial phagocytosis with subsequent cell apoptosis after PS-MPs treatment of HMC-3 cells. (a) Representative images of live cells captured during 24 h of PS-MPs treatment of HMC-3 cells. Blue arrows indicate microglial phagocytosis, green arrows indicate morphological changes to microglia cells, and red arrows point to early apoptotic morphological changes to HMC-3 cells. Scale bar = 50 μm. (b) Representative images of HMC-3 cells treated with 0.2 or 2 μm PS-MPs for 24 h. Green arrows indicate swollen amoeboid morphology and red arrows indicate apoptotic morphology of microglial cells. Scale bar = 100 μm. (c) Representative images of apoptosis analysis examined by BD Accuri C6 flow cytometer. Annexin-V^+ and PI^- cells are labelled as early apoptotic cells and Annexin-V^+ and PI^+ cells are labelled as late apoptotic cells. (d) Cell population ratios of early and late apoptotic cells from apoptosis analysis. (e) Representative images of western blotting for HMC-3 cells treated with PBS, 0.2 or 2 μm PS-MPs for 24 h. Protein expression of survivin, Bax, PARP, cleaved-PARP, Caspase8, −3, cleaved-Caspase8, −3, and β-actin were examined. β-actin was used as a loading control. (f) Representative images of the apoptotic fluorescent cells after 8 or 24 h 0.2 or 2 μm PS-MPs treatment. Blue indicates live cells, yellow or red indicates PS-MPs particles, and green indicates apoptotic region. Scale bar = 50 μm. $^{***}p < 0.001$ compared to the control group.

(Fig. 4B). To further confirm how the activation of immune response signals affects cytokine release, we measured mRNA expression levels of several cytokine genes. In PS-MP-treated HMC-3 cells, the mRNA expression levels of *IL-1β*, *CCL2*, and *TGF-β* were significantly decreased (Fig. 4C). Additionally, we conducted microarray analysis of HMC-3 cells using different concentrations (2.5, and 10 μg/mL) of the PS-MP mixture (Fig. 4D). We confirmed that genes related to immune responses, immunoglobulin genes, and microRNAs were altered by PS-MP treatment of HMC-3 cells. These results indicated that PS-MPs treatment affects microglial activation, which eventually leads to polarization and immune response gene transcription by HMC-3 cells.

3.5. Oral PS-MP treatment differentially affects murine microglial activation and apoptosis

Our findings surrounding *in vitro* PS-MP treatment displayed various facets involving increases in both microglial activation and cellular apoptosis. We sought to examine *in vivo* PS-MPs treatment at two different time points: 1 d and 7 d. To that end, we compared microglial cell type markers, immune responses, and apoptosis-related protein expression in brain tissue dissected at 1 d or 7 days after oral administration of PS-MPs. The brains of PS-MP-treated mice displayed a slight gradual decrease in Iba1 and CD206 expression, whereas the expression levels of CD68 and CD16 were moderately increased or unchanged (Fig. 5A). In contrast, after 7 d, PS-MP-treated mouse brains showed a critical diminishing pattern for all of the microglial cell markers, including Iba1, CD68, CD16, and CD206, suggesting an overall decrease in microglial cell numbers following PS-MP treatment (Fig. 5B). Moreover, 1 and 7 d PS-MP-exposed brains displayed different STAT3 and NF-κB expression patterns, while 1 d PS-MP-treated brains showed slightly diminished activation of phospho-STAT3 and a general decrease in NF-κB and its phosphorylation (Fig. 5C). Phosphorylation of both STAT3 and NF-κB was gradually increased by PS-MPs treatment (Fig. 5D). This countertrend between the two groups of PS-MP-treated brains was also observed in the western blot data for apoptotic markers. The levels of pro-apoptotic markers, including Bax, cleaved-PARP, cleaved-Caspase8, and cleaved-Caspase3, tended to decrease after PS-MPs treatment, whereas those of 7 d-exposed brains were markedly increased (Fig. 5E, F). In addition, expression of the anti-apoptotic marker survivin from the seven days sample was gradually elevated, while that of the one-day samples was unchanged (Fig. 5E, F). Finally, our data suggested that PS-MP exposure affected microglial phagocytosis and relevant cellular response activity, eventually leading to apoptosis.

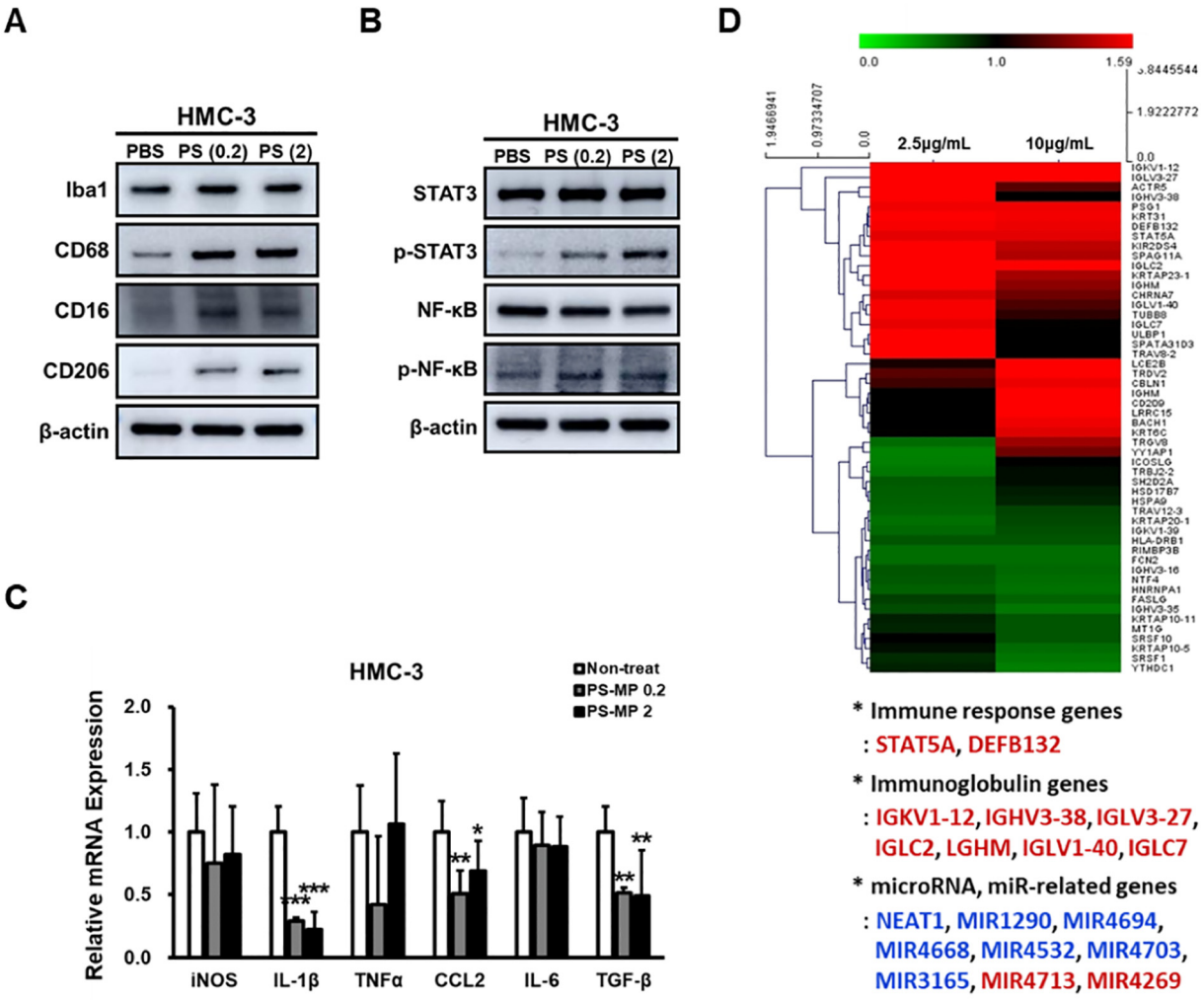

Fig. 4. Microglial activation and immune responses in HMC-3 cells after 24 h PS-MPs treatment. (a) Representative images of western blotting of HMC-3 cells treated with PBS, 0.2 or 2 μm PS-MPs for 24 h. Protein expression of Iba1, CD68, CD16, CD206, and β-actin were measured. β-actin was used as a loading control. (b) Representative images from western blotting data of PBS, 0.2 or 2 μm PS-MPs treated HMC-3 cells. Protein expression of STAT3, phospho-STAT3, NF-κB, phospho-NF-κB, and β-actin were measured. β-actin was used as a loading control. (c) Relative mRNA expression of *iNOS, IL-1β, TNF-α, CCL2, IL-6*, and *TGF-β* in HMC-3 cells treated with PBS, 0.2 or 2 μm PS-MPs for 24 h. *GAPDH* was used as a normalization control. (d) Heat map of differentially expressed gene values in HMC-3 cells treated with PBS, 2.5 or 10 μg/mL of mixed PS-MPs for 24 h. $^{*}p < 0.05$, $^{**}p < 0.01$, $^{***}p < 0.001$ compared to the control group.

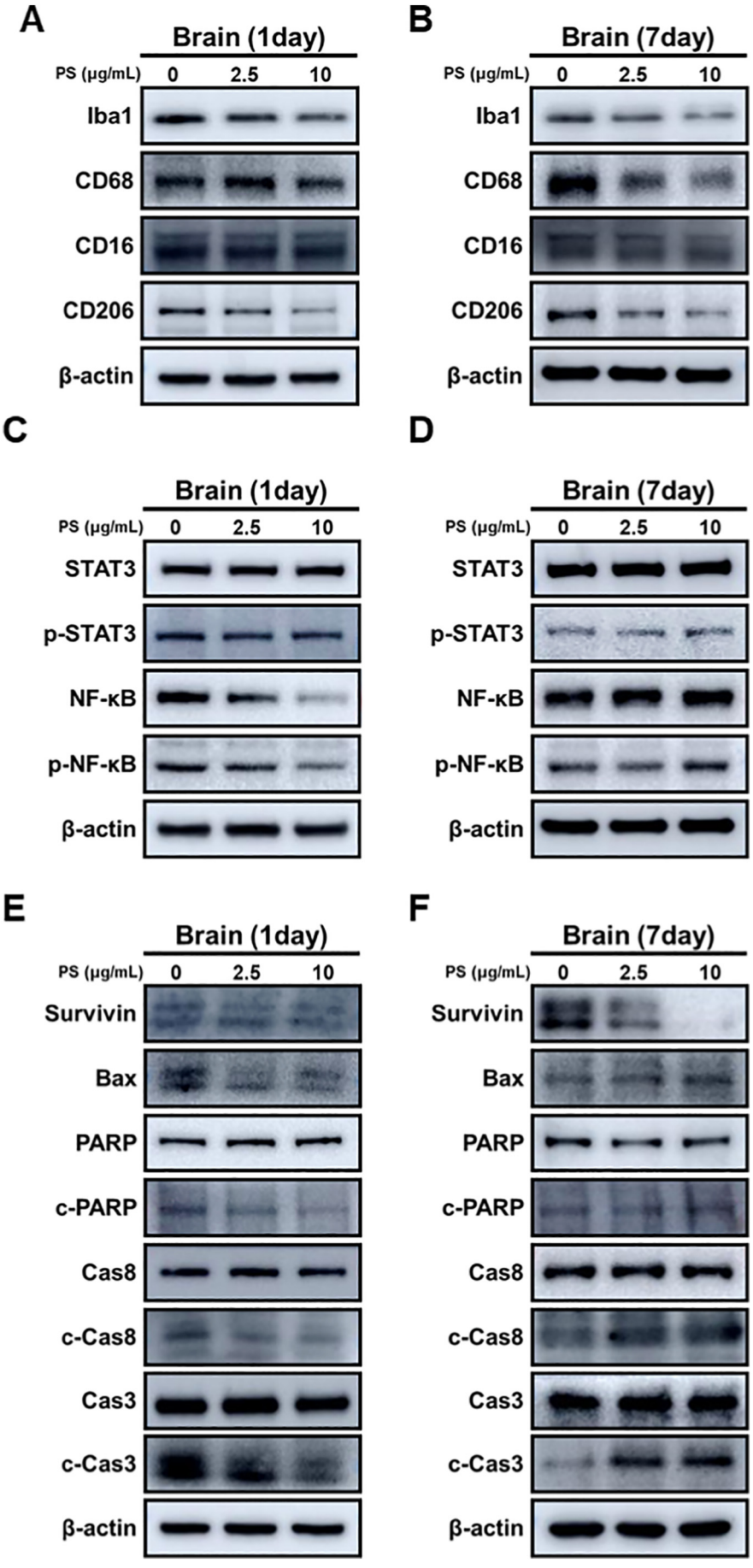
A
Brain (1day)
PS (μg/mL) 0 2.5 10
Iba1
CD68
CD16
CD206
β-actin
B
Brain (7day)
PS (μg/mL) 0 2.5 10
Iba1
CD68
CD16
CD206
β-actin
C
Brain (1day)
PS (μg/mL) 0 2.5 10
STAT3
p-STAT3
NF-κB
p-NF-κB
β-actin
D
Brain (7day)
PS (μg/mL) 0 2.5 10
STAT3
p-STAT3
NF-κB
p-NF-κB
β-actin
E
Brain (1day)
PS (μg/mL) 0 2.5 10
Survivin
Bax
PARP
c-PARP
Cas8
c-Cas8
Cas3
c-Cas3
β-actin
F
Brain (7day)
PS (μg/mL) 0 2.5 10
Survivin
Bax
PARP
c-PARP
Cas8
c-Cas8
Cas3
c-Cas3
β-actin

4. Discussion

To better understand the somewhat perplexing physiological responses in the brain against MP uptake, we investigated PS-MP deposition and ensuing immunological and molecular changes in PS-MP-treated mice and human microglial HMC-3 cells. Our findings suggested the hazardous potential of PS-MP ingestion in the brain, as supported by other recent reports (Jung et al., 2020; Prüst et al., 2020; Sarasamma et al., 2020; Sökmen et al., 2020).

In recent years, an increasing number of studies have attempted to define the toxicity of MPs in various mammalian cell types. Cells originating from primarily exposable organs, such as A549 cells from the lung, intestinal Caco-2 cells, or other blood cell types such as THP-1, U937, and peripheral blood monocytic cells (PBMC), were mainly examined upon PS-MP ingestion (Prietl et al., 2014; Stock et al., 2019; Xu et al., 2019). Many of these studies were largely based on the crucial question of whether MPs have detrimental effects on target cells. Step forward from these studies, there have been increasing number of studies showing the neurotoxic effects of MPs in mammalians; aquatic model studies showed diverse behavioral changes including hyperactivity or motor dysfunction, mammalian cell studies proved the MPs absorption and neurotoxic response, and these raised the possibility of neurotoxic effects against MPs exposure such as elevation of neuronal disorder vulnerability or changes in brain-gut-microbiota (Deng et al., 2018; Estrela et al., 2021; Huang et al., 2021; Prüst et al., 2020). Our study demonstrated that the brain could be another primary organ affected by PS-MP ingestion. Through the seven days of daily oral treatment with PS-MPs in mice, we presented the possibility of microglial accumulation of ingested PS-MPs in the brain. In addition, using three types of PS-MPs, we analyzed PS-MPs uptake in microglial cells and confirmed microglial phagocytosis of PS-MPs < 2 μm in size. The microglial phagocytic capacity for PS-MPs in our study corresponded with that of previous studies (Prietl et al., 2014; Stock et al., 2019). Considering the major phagocytic role of microglia in the brain and the existence of assorted phagocytic cells in many other organs, it is thought that cellular PS-MPs uptake in many organs, including the brain, is highly associated with local phagocytic activity in each region. Since the brain have their own specialized protective blood-brain barrier (BBB), the precise mechanism for PS-MPs penetrating through BBB have to be further investigated. Base on some previous studies about nanoparticles and their BBB penetration, it is assumed that PS-MPs might be penetrated through serum albumin or iron adsorptive-mediated transcytosis mediated by caveolae or clathrin (Brown et al., 2020; Hillaireau and Convreur, 2009). Nonetheless, the precise processes underlying PS-MPs delivery to the brain should be further investigated.

After 24 h of PS-MPs treatment of HMC-3 cells, we aimed to mimic the conditions of PS-MPs exposure and investigate the early responses of microglial cells to PS-MPs ingestion. Our study yielded interesting results. Despite the significant increase in apoptotic cell numbers (Fig. 3), PS-MP-treated HMC-3 cells displayed markedly elevated cell proliferation, microglial activation and differentiation markers, and immune response protein activation (Fig. 4). These *in vitro* data are, in some part, consistent with that of 1 d PS-MP-treated brains. One day PS-MP-treated brains displayed increased or maintained microglial activation marker CD68 and M1 type differentiation marker CD16 expression, while there was a slight decrease in total microglial marker Iba1 and M2 type differentiation marker CD206 expression. This implies that microglia in orally PS-MP-treated mouse brains were also activated but eventually perturbed the uptake of PS-MPs. Microglial cell type markers and apoptotic marker expression data from 7 d-treated brains also supported this; all four types of microglial markers were substantially diminished, whereas apoptotic marker changes were clearly proven to increase apoptosis after 7 d of PS-MPs ingestion. In addition, we identified activation of STAT3 and NF-κB, changes in several cytokine levels, such as IL-1β, CCL-2, and TGF-β, with transcriptional changes involving several gene clusters responsible for immune responses and immunoglobulins in PS-MP-treated HMC-3 cells. However, the expression patterns of STAT3, and NF-κB, and their phosphorylated proteins in the brains of the two groups of mice did not change significantly. Regarding the number of other cell types in the brain that were not directly affected by ingested PS-MPs, it is speculated that the effect of PS-MPs on the phosphorylation of transcriptional regulators of the whole brain were minor. Nevertheless, the physiological changes investigated in our *in vivo* oral PS-MPs administration experiments suggest a potential risk resulting from chronic ingestion of PS-MPs.

As we aimed to mimic and synchronize the PS-MPs exposure condition *in vitro* and *in vivo*, there are still several limitation and enigmatic points remained in our study. Since we have clarify the microglial phagocytosis of PS-MPs size under 2 μm (Fig. 2A), the cell viability data of HMC-3 cells against 10 μm PS-MPs 48 and 72 h treatment is questionable (Fig. 2B). Considering the impossibility of phagocytic microglial function against 10 μm PS-MPs and their adherent cell growing character, it is speculated that the proper proliferation of HMC-3 cells might be somehow obstructed by the spatial interruption occurred by consecutive PS-MPs treatment. However, the effect of 10 μm PS-MPs exposure to microglia may not be occurred *in vivo*, as we mentioned above about the BBB-penetrative size of PS-MPs is under 2 μm (Brown et al., 2020; Hillaireau and Convreur, 2009). Moreover, as our study did not clearly showed whether PS-MPs can be eliminated by microglial phagocytosis and they can affect surrounding neurons or astrocytes, the hazardous effect of PS-MPs-ingested microglia on nearby cells is worth of prospective study.

Since there have been a number of studies reporting that environmental PS-MPs are contaminated with diverse toxic chemicals, such as persistent organic pollutants, organochlorine pesticides, heavy metal ions, and so on, it is necessary to investigate the mammalian brain and microglial response against exposure to PS-MPs and absorption of these toxic chemicals (Ma et al., 2020; Mammo et al., 2020; Thomas et al., 2021). Moreover, as many studies focus on different types of MPs or characters including shape, surface charge, and so on (Hwang et al., 2019; Hwang et al., 2020; Choi et al., 2021), further diversified study will be necessary.

Taken together, we found that small-sized PS-MPs can accumulate in the brain through microglial phagocytosis and induce immune activation, which finally proceeds to the apoptotic process. These alterations in microglial cells raise the potential that chronic PS-MP ingestion could lead to adverse consequences in the brain. Our study represents a step forward in understanding the fundamental phenomenon of PS-MPs ingestion and their adverse effects in the brain.

5. Conclusions

In this era of MP pollution, there are growing concerns regarding the risk of MPs to our health. Despite an increasing number of studies regarding the adverse effects of MPs, the effect of PS-MPs in the brain have not yet been clearly investigated. Our study confirmed that a week of oral treatment with PS-MPs < 2 μm in size was sufficient for brain accumulation *via* microglial phagocytosis. It also provides evidence that PS-MP uptake induces microglial immune activation, which eventually leads to apoptosis. Further studies are underway to

Fig. 5. Alteration of microglial activity markers, immune response proteins, and apoptotic markers in mouse brain after 1 or 7 days oral PS-MPs treatment. (a–b) Representative images of western blotting presenting protein expression of Iba1, CD68, CD16, CD206, and β-actin from 1 d (a) or 7 d (b) Oral PS-MP-treated mouse brain. (c–d) Representative western blotting data for STAT3, phospho-STAT3, NF-κB, phospho-NF-κB, and β-actin from 1 d (c) or 7 d (d) Oral PS-MP-treated mouse brain. (e–f) Representative images showing protein expression of survivin, Bax, PARP, cleaved-PARP, Caspase8, −3, cleaved-Caspase8, −3, and β-actin from 1 d (e) or 7 d (f) Oral PS-MP-treated mouse brain. β-actin was used as a loading control.

elucidate the precise mechanisms underlying PS-MPs delivery to the brain, and to better understand brain and microglial responses to PS-MPs ingestion using PS-MPs containing toxic chemicals, thereby mimicking environmentally contaminated PS-MPs.

CRediT authorship contribution statement

Conceptualization, WK, DK, SJL, and SKC; Methodology, WK, DK, HYK, SWJ, SGL, HCK, JEH, and JKP; Investigation, WK, DK, HYK, YJL, MKK, JSH, JEH, and JKP; Formal analysis, WK, DK, HYK, YJL, MKK, and JSH; data curation, WK and DK; manuscript writing, WK, DK, SJL, and SKC; Supervision, SWJ, SGL, HCK, SJL, and SKC; All authors have reviewed and agreed to manuscript submission.

Declaration of competing interest

The authors declare no potential conflicts of interest.

Acknowledgements

This research was supported by the DGIST R&D Program of the Ministry of Science and ICT (2020010096).

References

Akanyange, S.N., Lyu, X., Zhao, X., Li, X., Zhang, Y., Crittenden, J.C., Anning, C., Chen, T., Jiang, T., Zhao, H., 2021. Does microplastic really represent a threat? A review of the atmospheric contamination sources and potential impacts. Sci. Total Environ. 777, 146020.

Barnes, D.K., Galgani, F., Thompson, R.C., Barlaz, M., 2009. Accumulation and fragmentation of plastic debris in global environments. Philos Trans. R. Soc. Lond. B Biol. Sci. 364, 1985–1998.

Brown, T.D., Habibi, N., Wu, D., Lahann, J., Mitragotri, S., 2020. Effect of nanoparticle composition, size, shape, and stiffness on penetration across the blood-brain barrier. ACS Biomater. Sci. Eng. 6 (9), 4916–4928.

Choi, D., Hwang, J., Bang, J., Han, S., Kim, T., Oh, Y., Hwang, Y., Choi, J., Hong, J., 2021. In vitro toxicity from a physical perspective of polyethylene microplastics based on statistical curvature change analysis. Sci. Total Environ. 142242.

Deng, Y., Zhang, Y., Qiao, R., Bonilla, M.M., Yang, X., Ren, H., Lemos, B., 2018. Evidence that microplastics aggravate the toxicity of organophosphorus flame retardants in mice (Mus musculus). J. Hazard. Mater. 357, 348–354.

Devriese, L.I., van der Meulen, M.D., Maes, T., Bekaert, K., Paul-Pont, I., Frère, L., Robbens, J., Vethaak, A.D., 2015. Microplastic contamination in brown shrimp (Crangon crangon, linnaeus 1758) from coastal waters of the southern North Sea and channel area. Mar. Pollut. Bull. 98, 179–187.

Estrela, F.N., Guimarães, A.T.B., Araújo, A.P.D.C., Silva, F.G., Luz, T.M.D., Silva, A.M., Pereira, P.S., Malafaia, G., 2021. Toxicity of polystyrene nanoplastics and zinc oxide to mice. Chemosphere 271, 129476.

Hillaireau, H., Convreur, P., 2009. Nanocarriers' entry into the cell: relevance to drug delivery. Cell. Mol. Life Sci. 66 (17), 2873–2896.

Hou, B., Wang, F., Liu, T., Wang, Z., 2021. Reproductive toxicity of polystyrene microplastics: in vivo experimental study on testicular toxicity in mice. J. Hazard. Mater. 405, 124028.

Hu, X., Leak, R.K., Shi, Y., Suenaga, J., Gao, Y., Zheng, P., Chen, J., 2015. Microglial and macrophage polarization-new prospects for brain repair. Nat. Rev. Neurol. 11, 56–64.

Huang, J.N., Wen, B., Xu, L., Ma, H.C., Li, X.X., Gao, J.Z., Chen, Z.Z., 2021. Micro/nano-plastics cause neurobehavioral toxicity in discus fish (Symphysodon aequifasciatus): Insight from brain-gut-microbiota axis.

Hwang, J., Choi, D., Han, S., Choi, J., Hong, J., 2019. An assessment of the toxicity of polypropylene microplastics in human derived cells. Sci. Total Environ. 684, 657–669.

Hwang, J., Choi, D., Han, S., Jeong, S.Y., Choi, J., Hong, J., 2020. Potential toxicity of polystyrene microplastic particles. Sci. Rep. 10 (1), 7391.

Jung, B.K., Han, S.W., Park, S.H., Bae, J.S., Choi, J., Ryu, K.Y., 2020. Neurotoxic potential of polystyrene nanoplastics in primary cells originating from mouse brain. Neurotoxicology 81, 189–196.

Lan, X., Han, X., Li, Q., Yang, Q.W., Wang, J., 2017. Modulators of microglial activation and polarization after intracerebral haemorrhage. Nat. Rev. Neurol. 13, 420–433.

Lee, Y.K., Hur, J., 2020. Adsorption of microplastic-derived organic matter onto minerals. Water Res. 187, 116426.

Li, B., Ding, Y., Cheng, X., Sheng, D., Xu, Z., Rong, Q., Wu, Y., Zhao, H., Ji, X., Zhang, Y., 2020. Polyethylene microplastics affect the distribution of gut microbiota and inflammation development in mice. Chemosphere 244, 125492.

Livak, K.J., Schmittgen, T.D., 2001. Analysis of relative gene expression data using real-time quantitative PCR and the 2(-Delta Delta C(T)) method. Methods 25, 402–408.

Lu, L., Wan, Z., Luo, T., Fu, Z., Jin, Y., 2018. Polystyrene microplastics induce gut microbiota dysbiosis and hepatic lipid metabolism disorder in mice. Sci. Total Environ. 631–632, 449–458.

Lu, Y., Zhang, Y., Deng, Y., Jiang, W., Zhao, Y., Geng, J., Ding, L., Ren, H., 2016. Uptake and accumulation of polystyrene microplastics in zebrafish (Danio rerio) and toxic effects in liver. Environ. Sci. Technol. 50, 4054–4060.

Ma, H., Pu, S., Liu, S., Bai, Y., Mandal, S., Xing, B., 2020. Microplastics in aquatic environments: toxicity to trigger ecological consequences. Environ. Pollut. 261, 114089.

Mammo, F.K., Amoah, I.D., Gani, K.M., Pillay, L., Ratha, S.K., Bux, F., Kumari, S., 2020. Microplastics in the environment: interactions with microbes and chemical contaminants. Sci. Total Environ. 743, 140518.

McCormick, M.I., Chivers, D.P., Ferrari, M.C.O., Blandford, M.I., Nanninga, G.B., Richardson, C., Fakan, E.P., Vamvounis, G., Gulizia, A.M., Allan, B.J.M., 2020. Microplastic exposure interacts with habitat degradation to affect behaviour and survival of juvenile fish in the field. Proc. Biol. Sci. 287, 20201947.

Mercogliano, R., Avio, C.G., Regoli, F., Anastasio, A., Colavita, G., Santonicola, S., 2020. Occurrence of microplastics in commercial seafood under the perspective of the human food chain. A review. 68, 5296–5301.

Prietl, B., Meindl, C., Roblegg, E., Pieber, T.R., Lanzer, G., Fröhlich, E., 2014. Nano-sized and micro-sized polystyrene particles affect phagocyte function. Cell Biol. Toxicol. 30, 1–16.

Prüst, M., Meijer, J., Westerink, R.H.S., 2020. The plastic brain: neurotoxicity of micro- and nanoplastics. Part. Fibre Toxicol. 17, 24.

Qiang, L., Cheng, J., 2021. Exposure to polystyrene microplastics impairs gonads of zebrafish (Danio rerio). Chemosphere 263, 128161.

Rivoira, L., Castiglioni, M., Rodrigues, S.M., Freitas, V., Bruzzoniti, M.C., Ramos, S., Almeida, C.M.R., 2020. Microplastic in marine environment: reworking and optimisation of two analytical protocols for the extraction of microplastics from sediments and oysters. MethodsX 7, 101116.

Rochman, C.M., Hoellein, T., 2020. The global odyssey of plastic pollution. Science 368, 1184–1185.

Sarasamma, S., Audira, G., Siregar, P., Malhotra, N., Lai, Y.H., Liang, S.T., Chen, J.R., Chen, K.H., Hsiao, C.D., 2020. Nanoplastics cause neurobehavioral impairments, reproductive and oxidative damages, and biomarker responses in zebrafish: Throwing up alarms of wide spread health risk of exposure. Int. J. Mol. Sci. 21.

Sharifinia, M., Bahmanbeigloo, Z.A., Keshavarzifard, M., Khanjani, M.H., Lyons, B.P., 2020. Microplastic pollution as a grand challenge in marine research: a closer look at their adverse impacts on the immune and reproductive systems. Ecotoxicol. Environ. Saf. 204, 111109.

Sökmen, T.Ö., Sulukan, E., Türkoğlu, M., Baran, A., Özkaraca, M., Ceyhun, S.B., 2020. Polystyrene nanoplastics (20 nm) are able to bioaccumulate and cause oxidative DNA damages in the brain tissue of zebrafish embryo (Danio rerio). Neurotoxicology 77, 51–59.

Stock, V., Böhmert, L., Lisicki, E., Block, R., Cara-Carmona, J., Pack, L.K., Selb, R., Lichtenstein, D., Voss, L., Henderson, C.J., Zabinsky, E., Sieg, H., Braeuning, A., Lampen, A., 2019. Uptake and effects of orally ingested polystyrene microplastic particles in vitro and in vivo. Arch. Toxicol. 93, 1817–1833.

Suman, T.Y., Jia, P.P., Li, W.G., Junaid, M., Xin, G.Y., Wang, Y., Pei, D.S., 2020. Acute and chronic effects of polystyrene microplastics on brine shrimp: first evidence highlighting the molecular mechanism through transcriptome analysis. J. Hazard. Mater. 400, 123220.

Sussarellu, R., Suquet, M., Thomas, Y., Lambert, C., Fabioux, C., Pernet, M.E., Le Goïc, N., Quillien, V., Mingant, C., Epelboin, Y., Corporeau, C., Guyomarch, J., Robbens, J., Paul-Pont, I., Soudant, P., Huvet, A., 2016. Oyster reproduction is affected by exposure to polystyrene microplastics. Proc. Natl. Acad. Sci. U. S. A. 113, 2430–2435.

Thomas, P.J., Perono, G., Tommasi, F., Pagano, G., Oral, R., Burić, P., Kovačić, I., Toscanesi, M., Trifuoggi, M., Lyons, D.M., 2021. Resolving the effects of environmental micro- and nanoplastics exposure in biota: A knowledge gap analysis. Sci. Total Environ. 146534.

Umamaheswari, S., Priyadarshinee, S., Bhattacharjee, M., Kadirvelu, K., Ramesh, M., 2020. Exposure to polystyrene microplastics induced gene modulated biological responses in zebrafish (Danio rerio). Chemosphere 128592.

Wang, X., Liu, L., Zheng, H., Wang, M., Fu, Y., Luo, X., Li, F., Wang, Z., 2020. Polystyrene microplastics impaired the feeding and swimming behavior of mysid shrimp Neomysis japonica. Mar. Pollut. Bull. 150, 110660.

Ward, J.E., Zhao, S., Holohan, B.A., Mladinich, K.M., Griffin, T.W., Wozniak, J., Shumway, S.E., 2019. Selective ingestion and egestion of plastic particles by the blue mussel (Mytilus edulis) and eastern oyster (Crassostrea virginica): implications for using bivalves as bioindicators of microplastic pollution. Environ. Sci. Technol. 53, 8776–8784.

Xie, X., Deng, T., Duan, J., Xie, J., Yuan, J., Chen, M., 2020. Exposure to polystyrene microplastics causes reproductive toxicity through oxidative stress and activation of the p38 MAPK signaling pathway. Ecotoxicol. Environ. Saf. 190, 110133.

Xu, M., Halimu, G., Zhang, Q., Song, Y., Fu, X., Li, Y., Li, Y., Zhang, H., 2019. Internalization and toxicity: a preliminary study of effects of nanoplastic particles on human lung epithelial cell. Sci. Total Environ. 694, 133794.

Yang, H., Lai, H., Huang, J., Sun, L., Mennigen, J.A., Wang, Q., Liu, Y., Jin, Y., Tu, W., 2020. Polystyrene microplastics decrease F-53B bioaccumulation but induce inflammatory stress in larval zebrafish. Chemosphere 255, 127040.

Yang, Y.F., Chen, C.Y., Lu, T.H., Liao, C.M., 2019. Toxicity-based toxicokinetic/toxicodynamic assessment for bioaccumulation of polystyrene microplastics in mice. J. Hazard. Mater. 366, 703–713.